Options to correct local turbulent flux measurements for large-scale fluxes using a LES-based approach

Matthias Mauder[1,5], Andreas Ibrom[2], Luise Wanner[1], Frederik De Roo[3], Peter Brugger[4], Ralf Kiese[1], Kim Pilegaard[2]

[1]Institute of Meteorology and Climate Research – Atmospheric Environmental Research, Karlsruhe Institute of Technology, 82467 Garmisch-Partenkirchen, Germany
[2]Dept. of Environmental Engineering, Technical University of Denmark (DTU), Kgs. Lyngby,2800, Denmark
[3]Development center for weather forecasting, Norwegian Meteorological Institute, 0313 Oslo, Norway
[4]Wind Engineering and Renewable Energy Laboratory (WiRE), École polytechnique fédérale de Lausanne (EPFL), CH-1015 Lausanne, Switzerland
[5]Institute of Hydrology and Meteorology, Technische Universität Dresden, 01062 Dresden, Germany

Formatiert: Hochgestellt

Correspondence to: Matthias Mauder (matthias.mauder@kit.edu)

Abstract. The eddy-covariance method provides the most direct estimates for fluxes between ecosystems and the atmosphere. However, dispersive fluxes can occur in the presence of secondary circulations, which can inherently not be captured by such single-tower measurements. In this study, we present options to correct local flux measurements for such large-scale transport based on a non-local parametric model that has been developed from a set of idealized ~~LES runs~~large-eddy simulations ~~for three real-world sites~~. Th~~is method is~~ tested for three real-world -sites DK-Sor, DE-Fen, and DE-Gwg, represent~~ing~~ typical conditions in the mid-latitudes with different measurement height, different terrain complexity and different landscape-scale heterogeneity. ~~Different~~ Two ways to determine the boundary-layer height, which is a necessary input variable for modelling the dispersive fluxes, are applied, either ~~from~~ based on operational radio-soundings and local in-situ measurements for the flat site or from backscatter-intensity profile obtained from collocated ceilometers for the two sites in complex terrain. The adjusted total fluxes are evaluated by assessing the improvement in energy balance closure and by comparing the resulting latent heat fluxes with evapotranspiration rates from nearby lysimeters. The results show that not only the accuracy of the flux estimates is improved but also the precision, which is indicated by RMSE values that are reduced by approximately 50%. Nevertheless, it needs to be clear that this method is intended to correct for a bias in eddy-covariance measurements due to the presence of large-scale dispersive fluxes. Other reasons potentially causing a systematic under- or overestimation, such as low-pass filtering effects and missing storage terms, still need to be considered and minimized as much as possible. Moreover, additional transport induced by surface heterogeneities is not considered.

1 Introduction

Eddy-covariance (EC) measurements provide fundamental data for the development of numerical models in meteorology, hydrology and biogeosciences. In order to produce accurate flux estimates, a series of physically-based corrections are usually

applied (Aubinet et al., 2012). Most of them are undisputed and are therefore used in standardized data processing strategies (Aubinet et al., 2000; Mauder et al., 2013; Sabbatini et al., 2018). Nevertheless, researchers typically find a general systematic

35 underestimation of the sum of the turbulent sensible and latent heat flux ($H + \lambda E$) by 10 to 30%, when these are validated against the available energy at the surface, i.e. the difference between net radiation and ground heat flux at the surface ($R_n - G_0$) (Hendricks-Franssen et al., 2009; Stoy et al., 2013; Wilson et al., 2002). Several studies indicate that the majority of this systematic bias is caused by dispersive fluxes, which arise from correlation of spatial variations of Reynolds mean variables and are influenced by the heterogeneity below the scale of the spatial averaging. Dispersive momentum fluxes are typically

40 neglected when applying a volume averaging operator to describe the turbulent flow in plant canopies (Lee, 2018). However, these dispersive fluxes can be significant in the context of the surface for the total transport above the canopy, where they are a result of secondary circulations (Mauder et al., 2020). These circulations develop under convective conditions and are superimposed on the mean flow. They comprise distinct phenomena, which are large-scale turbulent organized structures over homogeneous surfaces and thermally induced mesoscale circulations over heterogeneous surfaces (Inagaki et al., 2006; Kanda

45 et al., 2004; Steinfeld et al., 2007). Both phenomena contribute to the transport of momentum and scalars between the surface and the atmosphere, but can inherently not be captured by single-tower measurements (Etling and Brown, 1993).

A number of correction methods have been tested in the past in order to compensate for this systematic bias by distributing the surface energy balance (SEB) residual, either entirely or almost entirely towards the sensible heat flux (e.g. Charuchittipan et al., 2014; Ingwersen et al., 2011), or according to the Bowen ratio (e.g. Mauder et al., 2013; Twine et al., 2000), or entirely to

50 the latent heat flux (e.g. Wohlfahrt et al., 2010). However, an evaluation of these different SEB closure adjustment options remained somewhat inconclusive as to which of the methods under investigation is preferable (Mauder et al., 2018). Now, a novel method is available that is, in contrast to the previous methods, physically-based and semi-empirical in character, meaning it relates the dispersive fluxes (which are causing a systematic bias in single-tower EC) to readily accessible meteorological variables, and the semi-empirical coefficients are determined from a systematic parameter study using large-

55 eddy simulations. the

non-dimensional, non-local scaling variables u_*/w_* and z/z_i, where u_* is the friction velocity, w_* is the convective velocity scale, z is the height above ground and z_i is the boundary-layer height. The resulting functional relationships are fitted to a set of large-eddy simulations (LES), thereby representing a deeper understanding of the underlying transport processes (De Roo et al., 2018). As a result, we obtain two different correction equations, one for H and one for λE:

60 $$H_{\text{disp}} = \frac{F_{1H}(u_*/w_*)F_{2H}(z/z_i)}{1 - F_{1H}(u_*/w_*)F_{2H}(z/z_i)} H_m, \tag{1}$$

$$\lambda E_{\text{disp}} = \frac{F_{1E}(u_*/w_*)F_{2E}(z/z_i)}{1 - F_{1E}(u_*/w_*)F_{2E}(z/z_i)} \lambda E_m, \tag{2}$$

where the index "disp" stands for dispersive, representing the dispersive flux contribution that needs to be added as a correction to the measured fluxes, as indicated by the index "m". Please note that this correction is only applicable to unstable

2

65

$$F_{1H} = 0.197 \exp(-17.0\ u_*/w_*) + 0.156 \quad\quad\quad (3)$$

$$F_{1E} = 0.224 \exp(-14.0\ u_*/w_*) + 0.071 \quad\quad\quad (4)$$

$$F_{2H} = 0.21 + 10.69\ z/z_i \quad\quad\quad (5)$$

$$F_{2E} = 0.27 + 9.99\ z/z_i \qu\quad\quad (6)$$

75

$$H_{tot} = H_m + \frac{H_{disp}}{(H_{disp} + \lambda E_{disp})}\ Res, \quad\quad\quad (7)$$

$$\lambda E_{tot} = \lambda E_m + \frac{\lambda E_{disp}}{(H_{disp} + \lambda E_{disp})}\ Res,$$

$$\quad\quad (8)$$

$$Res = (H_m + \lambda E_m)\left(\frac{1}{EBR_d} - 1\right), \quad\quad\quad (9)$$

In this study, we will present a first real-world application of this new SEB closure correction method. More specifically, we
will apply the method to data from three different EC sites with different site characteristics, such as canopy height, surface
heterogeneity and terrain complexity. One of these sites is a tall forest with an aerodynamic measurement height of 23 m, so
that the absolute magnitude of the correction can be evaluated by comparing the overall SEB closure before and after the

85 correction. For two other sites, we will compare the resulting estimates for the latent heat flux with independently measured
lysimetric evapotranspiration (ET) measurements. This will allow us to address the following two research questions:

1. How realistic is the partitioning approach of the SEB residual into latent and sensible heat flux fractions?
2. How well can the absolute magnitude of the correction be estimated?

3

We will now present further details about these three test sites, including their instrumentation and data processing chain in section 2, followed by the results in section 3. Then, we will discuss the implications of our findings including the possibility to use this method for other sites in section 4 before we summarize our conclusions in section 5.

2 Methodology

2.1 The semi-empirical energy balance adjustment method

The method proposed by De Roo et al. (2018) relates the dispersive fluxes, and hence the energy imbalance, to the non-dimensional, non-local scaling variables u_*/w_* and z/z_i, where u_* is the friction velocity, w_* is the convective velocity scale, z is the height above ground and z_i is the boundary-layer height. The resulting functional relationships are fitted to a set of large-eddy simulations (LES), thereby representing ~~a deeper understanding of~~ the underlying transport processes (De Roo et al., 2018). As a result, ~~we obtain~~ two different correction equations are obtained, one for H and one for λE:

$$H_{\text{disp}} = \frac{F_{1H}(u_*/w_*)F_{2H}(z/z_i)}{1-F_{1H}(u_*/w_*)F_{2H}(z/z_i)} H_m \tag{1}$$

$$\lambda E_{\text{disp}} = \frac{F_{1E}(u_*/w_*)F_{2E}(z/z_i)}{1-F_{1E}(u_*/w_*)F_{2E}(z/z_i)} \lambda E_m \tag{2}$$

where the index "disp" stands for dispersive, representing the dispersive flux contribution that needs to be added as a correction to the measured fluxes, as indicated by the index "m". Please note that this correction is only applicable to unstable stratification, i.e. when the Obukhov length $L < 0$, because secondary circulations and the associated dispersive fluxes are restricted to these conditions. F_{1H}, F_{2H}, F_{1E}, and F_{2E} are semi-empirical functions:

$$F_{1H} = 0.197 \exp(-17.0\ u_*/w_*) + 0.156 \tag{3}$$

$$F_{1E} = 0.224 \exp(-14.0\ u_*/w_*) + 0.071 \tag{4}$$

$$F_{2H} = 0.21 + 10.69\ z/z_i \tag{5}$$

$$F_{2E} = 0.27 + 9.99\ z/z_i \tag{6}$$

These constants were derived by De Roo et al. (2018) as the results of a curve-fitting to their model output. Due to the limited grid resolution of the LES, which employed a grid spacing of 5 m in the horizontal and 2 m in the vertical direction, these functions cannot be expected to hold for measurement heights by z_m below 20 m. In this case, De Roo et al. (2018) suggest that the correction is scaled by the daily energy balance ratio EBR_d, analogously to the method of Mauder et al. (2013). Nevertheless, the partitioning of the residual is based on the LES parameter study of De Roo et al. (2018):

$$H_{tot} = H_m + \frac{H_{disp}}{(H_{disp}+\lambda E_{disp})}\ Res \tag{7}$$

4

$$\lambda E_{tot} = \lambda E_m + \frac{\lambda E_{disp}}{(H_{disp} + \lambda E_{disp})} \, Res .$$

$$\tag{8}$$

$$Res = (H_m + \lambda E_m)\left(\frac{1}{EBR_d} - 1\right). \tag{9}$$

where the index "tot" stands for the total corrected heat flux and the variable *Res* stands for the SEB residual based on independent field measurements, assuming that dispersion is the only significant cause for the SEB imbalance.

2.1 2 Soroe beech forest site (DK-Sor)

The Soroe beech forest site (DF-Sor) is located in the central part of the Danish island of Zealand (55.4858694° N, 11.6446444° E, 40 m AMSL). It is surrounded by flat but heterogeneous terrain, which is characterized by a land-cover mix comprising forests, agricultural area and small settlements (Figure 1). The beech forest around the EC tower is called "Lille Boegeskov", which extends approximately 2.4 km in N-S direction and approximately 1.0 km in E-W direction. The forest itself is also heterogeneous, as some smaller patches inside this beech forest are covered with other species, mostly plantations of coniferous trees. Another larger beech forest, which is located to the Northeast of the EC tower (Figure 1), may also contribute to the flux footprint at times, depending on wind direction and atmospheric stability.

130   **Figure 1: Aerial image of the DK-Sor site. Beech forest is indicated by a polygon with a green edge and the exclusion areas, i.e. patches of coniferous trees, inside the Lille Boegeskov beech forest are indicated by polygons with a white edge, © Google Earth.**

2.~~1~~2.1 Micrometeorological measurements

The EC-System is still very similar to the one developed in 1993 and operating since then at this site. A main feature is the

135   long sampling tube that allows keeping the IRGA (LI-7000, Li-Cor, Lincoln, Nebraska, USA) in a temperature-controlled hut close to the base of the 45 m tower. Since 2013, a Gill HS50 sonic anemometer is used at $z_m = 43.6$ m. The net-radiometer is a combination of a pyrgeometer (CG4, Kipp & Zonen, Delft, The Netherlands) and a pyranometer (CM11, Kipp & Zonen) each pointing both upwards and downwards. Contrary to the new ICOS set-up the devices are not ventilated. For details, see Tab. 1 in Pilegaard and Ibrom (2020). Ground heat flux was observed with two self-calibrating heat flux plates (HFP01SC,

140   Thermal Sensors BV, Delft, The Netherlands). The eddy covariance raw data were processed as described in Pilegaard and Ibrom (2020), applying the humidity dependent spectral dampening correction following Ibrom et al, (2007), but with a co-spectral integration method of the total transfer function based on co-spectral models from Horst (1997) to calculate the flux correction factor. The raw data were first processed with the software rcpm, developed by A. Ibrom, resulting in covariances and variances. Further flux corrections and quality control were applied by using custom made R-scripts. The data set used for

145   this study covers period from 1 April until 31 December 2018.

Figure 2: Photograph of the 45 m mast and the nearby scaffolding tower at the DK-Sor beech forest site (photograph by Kim Pilegaard).

2.~~1~~2.2 Determination of the boundary-layer height

For the determination of the boundary-layer height at Soroe, we applied the method of Batchvarova and Gryning (1990), which relies on friction velocity u_*, sensible heat flux H, and air density measured at the DK-Sor station. In addition, radio sounding data for determining the morning temperature gradient in the free atmosphere were obtained from the worldwide repository hosted at the University of Wyoming (http://weather.uwyo.edu/upperair/sounding.html) for the station Schleswig (station number 10035), which is located about 170 km west of this site. Despite the distance, it is the closest permanent radio sounding station available, and it has a similar topographic setting as Soroe, so it is reasonable to assume the temperature gradient above the boundary layer being similar. Based on these data, we calculated the potential temperature difference between the heights of 1500 m and 500 m for the 6 UTC sounding on all days of the observation period.

2.~~1~~2.3 Determination of the flux footprint

The flux footprint for the DK-Sor site was calculated for every 30-min averaging interval for the entire observation period by using the simple two-dimensional parametric model (FFP) by Kljun et al. (2015). Besides the measurement height z_m, this model requires 30-min data for the horizontal wind speed at the measurement height $u(z_m)$, friction velocity u_*, the Obukhov length L, and the standard deviation of the cross-wind component σ_v as input variables, which were readily available from the EC system. In addition, the model requires z_0, which was set to a fixed value of 1.80 m, and z_i for every 30 min interval, which was determined according to the method of Batchvarova and Gryning (1990) as explained in section 2.1.2. The resulting flux contributions from beech forest to the footprint of the DK-Sor EC dataset are presented in Figure 3 in form of a histogram. The most common flux contribution class is from 0.7 to 0.75, meaning the 70% to 75% of the respective 30-min flux originates from an area covered with beech forest based on a land cover map covering an area ~~pf~~ of 4x4 km² centred around the tower. The median lies at a value of 0.704, meaning that in 50% of the 30-min intervals, more than 70.4% of the measured flux consists of flux contributions from the beech forest. The average source contribution from beech forest is 75.6%.
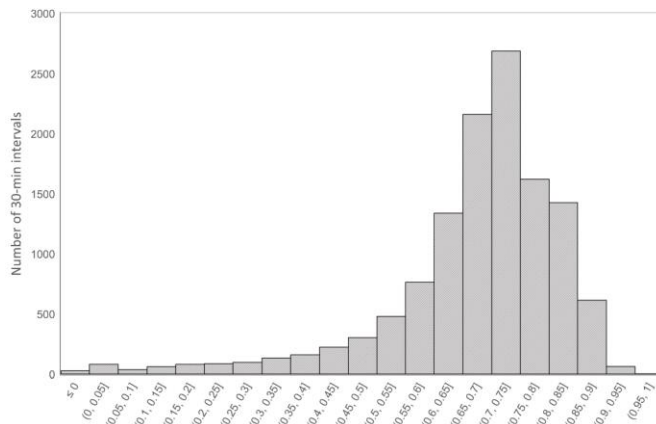
Figure 3: Histogram of the flux footprint contributions of beech forest to the EC measurements at DK-Sor during the observation period from 1 April to 31 December 2018. Note that this dataset comprises all valid 30-min intervals, while the energy balance closure correction method is only applied for those with $z_i/L < 0$.

The DK-Sor dataset comprised a total of 12469 30-min values. From those, 6572 values fulfilled the criterium of $z_i/L < 0$ of the De Roo et al. (2018) method and presence all four main components of the energy balance, so that the energy balance

8

180 closure correction method could be applied. This dataset was then filtered using a threshold of 75% flux contributions from beech forest according to the quality requirements of Mauder et al. (2013). The number of measured data was further reduced from 6572 to 4834, i.e. by 26%, due to the footprint filtering.

2.2 3 TERENO Pre-Alpine grassland sites (DE-Fen, DE-Gwg)

185 The two sites DE-Fen (Fendt, 47.8329° N 11.0607° E, 595 m AMSL) and DE-Gwg (Graswang, 47.5708° N 11.0326° E, 864 m AMSL) are located at flat valley-bottoms in the TERENO (Terrestrial Environmental Observatories) Pre-Alpine Observatory, S-Germany. The DE-Fen site is surrounded by mildly complex terrain with differences in altitude on the order of 100 m while the DE-Gwg site is located in an area with differences in altitude on the order of 1000 m. The valley-bottoms in this region are usually grasslands, partially either managed as pasture and or as meadow and the slopes are often covered
190 with forests up to the timberline. Both sites were chosen in a way so that their fetch is homogeneous and flat in all directions within a radius of 200 m, so that most of the flux contributions can be assumed to originate from grassland, which is the target land use type. This has also been demonstrated through footprint calculations by Soltani et al. (2018).

2.2 3.1 Micrometeorological measurements

The instrumentation of the EC-systems at DE-Fen (Figure 4) and DE-Gwg (Figure 5) is nearly identical, comprising a CSAT3
195 sonic anemometer (Campbell Sci. Inc, Logan, UT, USA) and a LI-7500 infrared gas analyzer (Li-Cor Inc, Lincoln, NE, USA) for measuring the sensible and latent heat flux. The measurement height is 3.5 m above ground level. Net radiation is measured at a height of 2 m above ground level by a four-component net-radiometer (CNR-4, Kipp&Zonen BV, Delft, The Netherlands) and ground-heat flux at the soil surface is measured by a combination of three self-calibration heat flux plates (HFP01SC), three soil temperature profiles (T106, Campbell Sci. Inc. Logan, UT, USA) and three soil water content profiles (CS616,
200 Campbell Sci. Inc., Logan, UT, USA) following the PlateCal method of Liebethal (2005), which is a combination of heat flux plate measurements and a calorimetric approach. Further details about the additional meteorological measurements at these sites can be found in Kiese et al. (2018).

The data processing follows the strategy for quality and uncertainty assessment of long-term EC measurements of Mauder et al. (2013). More specifically, we applied the double rotation method to align the coordinate system into the mean streamlines
205 (Kaimal and Finnigan, 1994). We corrected for humidity fluctuations in the sensible heat flux measurement according to Schotanus et al. (1983). We compensated for spectral losses according to the method of Moore (1986) and corrected the latent heat flux for density fluctuations following Webb et al. (1980). EC data were screened for steady-state conditions and well-developed turbulence according to a modified version of the method of Foken and Wichura (1996). The measurement period for this study is one entire year from 1 January until 31 December 2014.

210

Figure 4: Photograph of the eddy-covariance system at DE-Fen grassland site. The hill in the background has a height of about 100 m compared to the grassland in the foreground (photograph by Matthias Mauder).

215

Figure 5: Photograph of the eddy-covariance system at DE-Gwg grassland site. The mountains in the background are up to 1000 m higher than the grassland in the foreground (photograph by Matthias Mauder).

No u_*-filtering was applied because a decoupling of the canopy layer from the air above was not considered to be likely for

220   these sites covered with short grass. However, the flux data are filtered using tests on well-developed turbulence and steady

state conditions (Foken et al., 2004; Foken and Wichura, 1996; Ruppert et al., 2006). In order to be able to compare the latent heat fluxes measured at the TERENO Pre-Alpine grassland EC sites with the collocated lysimeters, daily sums of ET were calculated. To this end, we applied the gap-filling approach of Reichstein (2005) based on a look-up table method by using the REddyProc software (Wutzler et al., 2018) in the same way as Mauder et al. (2018) did this for an earlier comparison of SEB
225 adjustment methods.

2.23.2 Determination of the boundary-layer height

A ceilometer of type CL51 (Vaisala Oyi, Vantaa, Finland) was deployed at each of the two TERENO Pre-Alpine stations DE-Gwg and DE-Fen. This instrument employs a pulsed diode laser LIDAR (Light Detection And Ranging) technology, where short, powerful laser pulses are sent out in a vertical or near-vertical direction. The reflection of light (backscatter) caused by
230 aerosols, clouds, precipitation or another obscuration is analyzed. Backscatter profiles, which are averaged over 10 min, are used to determine the boundary-layer height based on the maximum gradient method CL51 (Emeis et al., 2011; Münkel et al., 2007). This method is based on the assumption of convective conditions, so that the aerosols are well-mixed throughout the boundary-layer, while their concentration decreases sharply in the free atmosphere. The resulting values for z_i were used as input for the energy balance closure correction method of De Roo et al. (2018), which is only applicable for unstable conditions,
235 meaning that during those periods also the assumptions for the boundary-layer height retrieval method can be considered to be fulfilled.

### 2.23.3 Lysimeter-measurements of evapotranspiration

As part of the TERENO SoilCan network the DE-Fen and DE-Gwg sites were equipped with fully automated lysimeter systems which are operated with standardized sensor installations and measuring design (Pütz et al., 2016) in close vicinity (<500m)
240 to the respective eddy covariance systems (see 2.2.1). At both sites, evapotranspiration was measured from weighable lysimeters (N=3) filled with intact soil cores (1 m², 1.4 m height), excavated at representative grassland locations in the surrounding of the EC stations (Kiese et al., 2018). Water fluxes from at the bottom of these closed lysimeters are regulated by adjusting matrix potential in 1.4 m (TS1, Meter Group, Munich, Germany) inside the lysimeter to match outside conditions measured in the same depth in the surrounding soil. If the water tension in the lysimeter is higher than outside conditions,
245 water is pumped into a weighable tank via an underpressurized suction rake (SIC40, Meter Group, Munich, Germany) and vice versa if the soil inside the lysimeter is drier than outside conditions. Grassland water fluxes of precipitation, evapotranspiration, and groundwater recharge are derived from precision weighting of each lysimeter with three load cells (Model 3510, Tedea-Huntleigh, Canoga Parl, CA, USA, precision of 10 g, equivalent to 0.01 mm water) and water tanks in 1-min time intervals. Time series of lysimeter and water tank weights were quality checked before post-processing by applying
250 the adaptive window and adaptive threshold filter for separation of signal and noise (Fu et al., 2017; Peters et al., 2014). Daily

11

evapotranspiration rates in millimetres were calculated by summing up minute-based negative weight changes of the lysimeters corrected by positive weight changes of water tanks representing lowering of lysimeter weights due to groundwater recharge.

3 Results

3.1 Case study not limited by z_m

255 First, we have a look at the dataset of DK-Sor (Figure 6), where the LES-based correction can be applied directly without the need to adjust the correction factor with the measured EBR_d because the aerodynamic measurement height z_m is larger than 20 m there. The SEB closure is already relatively good on average in comparison with other sites with a slope of 0.94 and an intercept of 3.26 W m^{-2} of an orthogonal Deming regression (Manuilova et al., 2014). The scatter around this regression line can be characterized by a Pearson's correlation coefficient r of 0.915. After application of the correction, the slope increases

260 to 0.99 and the intercept stays almost the same with a value of 3.92 W m^{-2}. Also, the Pearson's r is even slightly increased with a value of 0.916. Overall, we can state that the SEB closure has clearly improved as a result of the correction with a regression line very close to identity. As expected from De Roo et al. (2018), we found that the relative contribution of dispersive fluxes to the total flux was larger for H than for λE, more specifically, H was increased by 6% on average and λE was increased by 4% on average. Please note that the correction is completely independent from measurements of the available

265 energy at the surface ($R_n - G$), the closeness of the regression line to the identity function is thus an empirical proof of the correction method. However, no alternative measurements of either ET or H are available for this beech forest site, so that we can only validate the sum of the turbulent fluxes but not their partitioning between H and λE here.
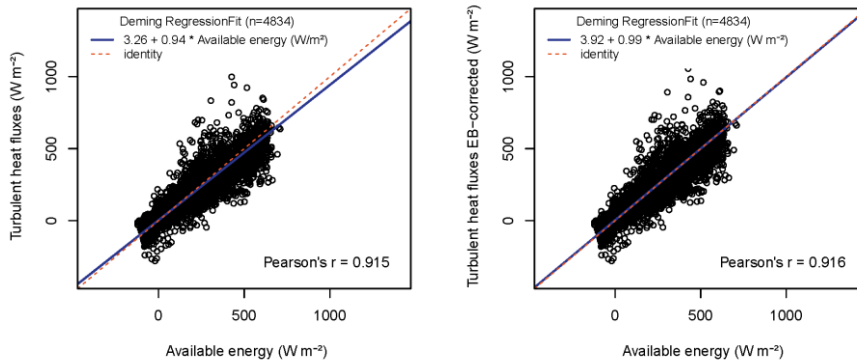
Figure 6: Results of the orthogonal regression analysis of the sum of the turbulent heat fluxes ($H + \lambda E$) vs. the available energy ($R_n - G$) as measured (left panel) and after application of the EBC correction (right panel) for the DK-Sor dataset.

12

270   In addition to this overall analysis of the energy balance closure, we also analyzed the seasonal variability of the mean diurnal cycle of the modelled dispersive fluxes in comparison with the measured residual (Figure 7). The agreement between both curves is reasonable during daytime with generally positive values of up to 50 W m^{-2}. The modelled dispersive fluxes peak already before noon local time, which is 1100 UTC, while the measured residual peaks later in the early afternoon, at least for the months from April to September. During nighttime, the modelled dispersive fluxes are generally small and nearly zero. In

275   contrast, the measured residual is often quite large and negative. This discrepancy reflects the fact that secondary circulations, and hence also the associated dispersive fluxes, are generally a phenomenon of the daytime convective boundary layer. At night, other processes obviously contribute largely to the overall SEB residual, e.g. advection or storage terms, which are not considered in the model by De Roo et al. (2018). When comparing the different seasons with each other, we find that the daytime dispersive fluxes are smaller in the months from October to December than between April and September, which can

280   probably be explained ~~with~~ by a combination of smaller sensible heat fluxes and less unstable conditions during this period of the year.
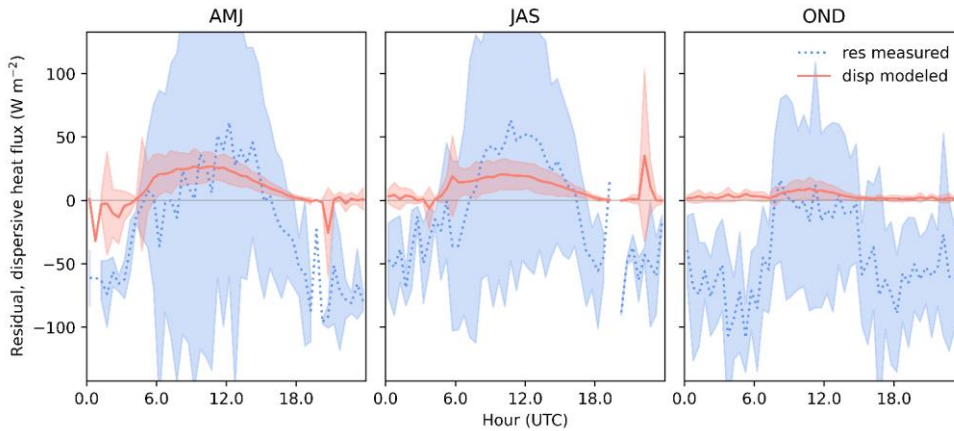
Figure 7: Mean diurnal cycles of the measured residual (blue) and the modelled dispersive fluxes (red) for different seasons (AMJ: April, Mai, June; JAS: July, August, September; OND: October, November, December) for the DK-Sor dataset. The semi-
285   **transparent blue and red areas represent the respective standard deviations.**

3.2 Case study limited by z_m

Next, we apply the LES-based SEB correction to the grassland datasets of DE-Fen and DE-Gwg. At both sites, the effective measurement heights were less than 20 m, so that the correction had to be adjusted by the measured EBR$_d$ (eq. 7-9). As a

290   result, the regression line after the correction is forced to be close to identity. And indeed, the regression slope is increased

13

from 0.77 to 1.04 for the DE-Fen data (Figure 8) and from 0.70 to 1.02 for the DE-Gwg data (Figure 9). For both sites, also the Pearsons's r increases by 0.02 as a result of the correction, which is a highly signicicant improvement. ~~r~~This is remarkable because it shows that this method also reduces the random error and not only a systematic bias. It can be seen in the original data that the closure is better at low energy fluxes, so that the data are slightly banana-shaped; this is nicely being corrected

295   for.

Please note that the number of valid data points n is reduced as a result of the correction by about 6-7% for both datasets, because we introduced two outlier criteria in order to avoid unrealistic fluxes when

    a) $EBR_d < 0.5$ and $EBR_d > 1.5$, and

    b) $|(H_{res} + \lambda E_{res})| < 0.01$ W m^{-2}.

300   The reduction in sample size is also one reason why the resulting regression slopes are slightly larger than one and not identical to one as expected after applying this correction. Another reason is the slightly negative intercept, which is caused by a few data points with a negative sum of the turbulent heat fluxes. Note that no correction was applied to these data points by this method because is only necessary for unstable stratification.
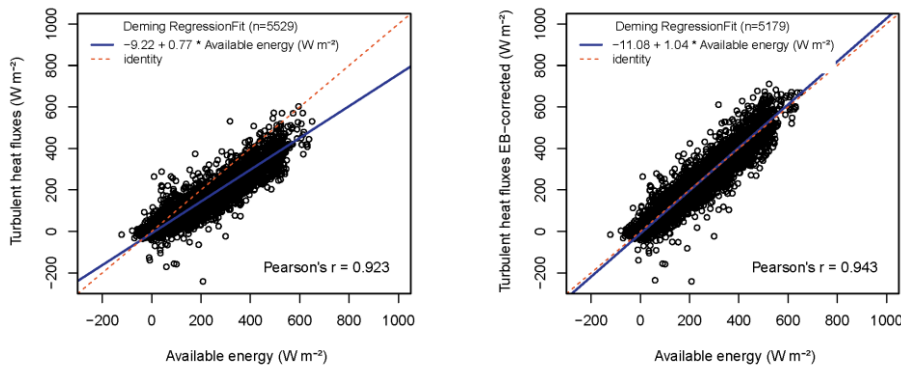
Figure 8: Results the orthogonal regression analysis of the sum of the turbulent heat fluxes ($H + \lambda E$) vs. the available energy ($R_n - G$) as measured (left panel) and after application of the EBC correction (right panel) for the DE-Fen dataset.
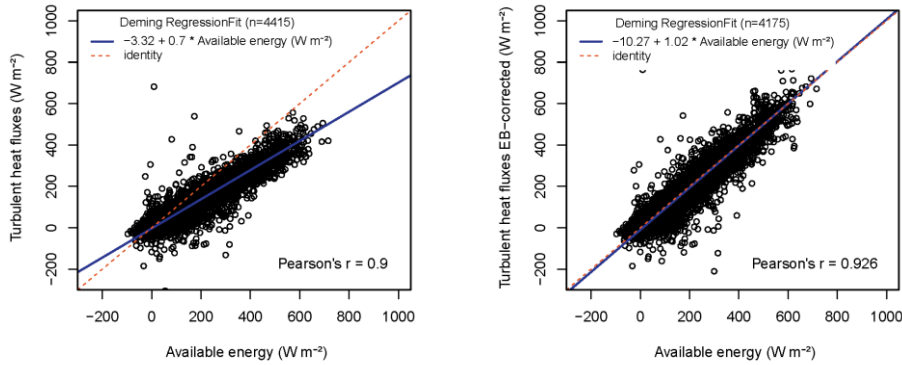
Figure 9: Results the orthogonal regression analysis of the sum of the turbulent heat fluxes ($H + \lambda E$) vs. the available energy ($R_n - G$) as measured (left panel) and after application of the EBC correction (right panel) for the DE-Gwg dataset.

3.3 Independent constraint on energy partitioning: water balance lysimeter

310   For the two grassland sites DE-Fen and DE-Gwg, the SEB closure correction needed to be scaled with the measured EBR due to the low measurement height. However, due to the nearby water balance lysimeters, we have the opportunity to test whether the partitioning of the SEB residual by this correction into the sensible and latent heat flux is realistic. To this end, we compared daily ET rates to four different options of correction for energy balance closure with these independent reference measurements; more specifically, these are

315   -   No correction to the latent heat flux, i.e the entire residual is attributed to the sensible heat flux (Ingwersen et al., 2011)

     -   Bowen-ratio preserving partitioning of the SEB residual according to the daily EBR_d (Mauder et al., 2013)

     -   Partitioning of the SEB residual according to the ratio between the sensible heat flux and the buoyancy flux forcing closure for every 30-min interval (Charuchittipan et al., 2014)

320   -   LES-based correction for dispersive fluxes (De Roo et al., 2018)

For DE-Fen, we clearly see from Figure 10 that the first option without any correction produces systematically too low ET rates that are characterized by a regression slope of 0.70 with a moderate scatter indicated by a Pearson's r of 0.908. In contrast, the Bowen-ratio preserving method leads to an overestimation of ET and a regression slope of 1.09, while the scatter is slightly reduced with the Pearson's r being increased from 0.908 of 0.915, which is not significant difference. The method of

15

325 Charuchittipan et al. (2014) produces by far the largest scatter and the lowest Pearson's r of 0.628, and the slope of 1.12 is even larger than that of the Bowen-ratio preserving method. Lastly, the LES-based method results in a slope of 0.9 and the highest Pearson's *r* of 0.937. This Pearson's *r* is significantly improved compared to the method of Mauder et al. at a level of p = 0.08 and at a much higher level of significance compared to the other two methods.
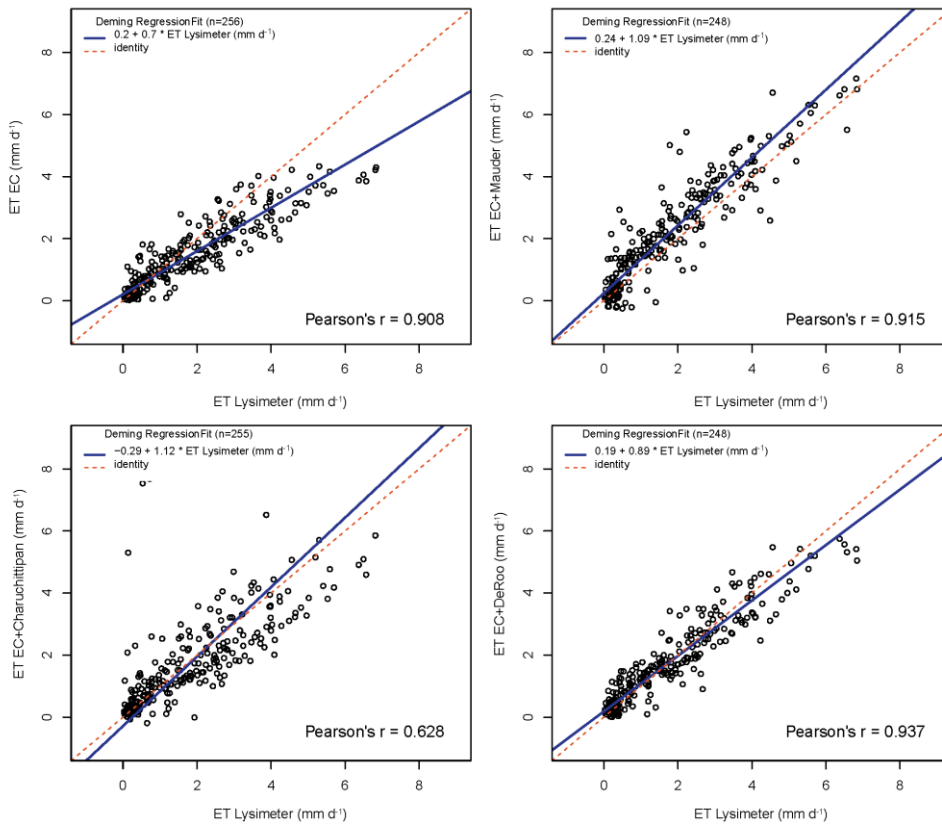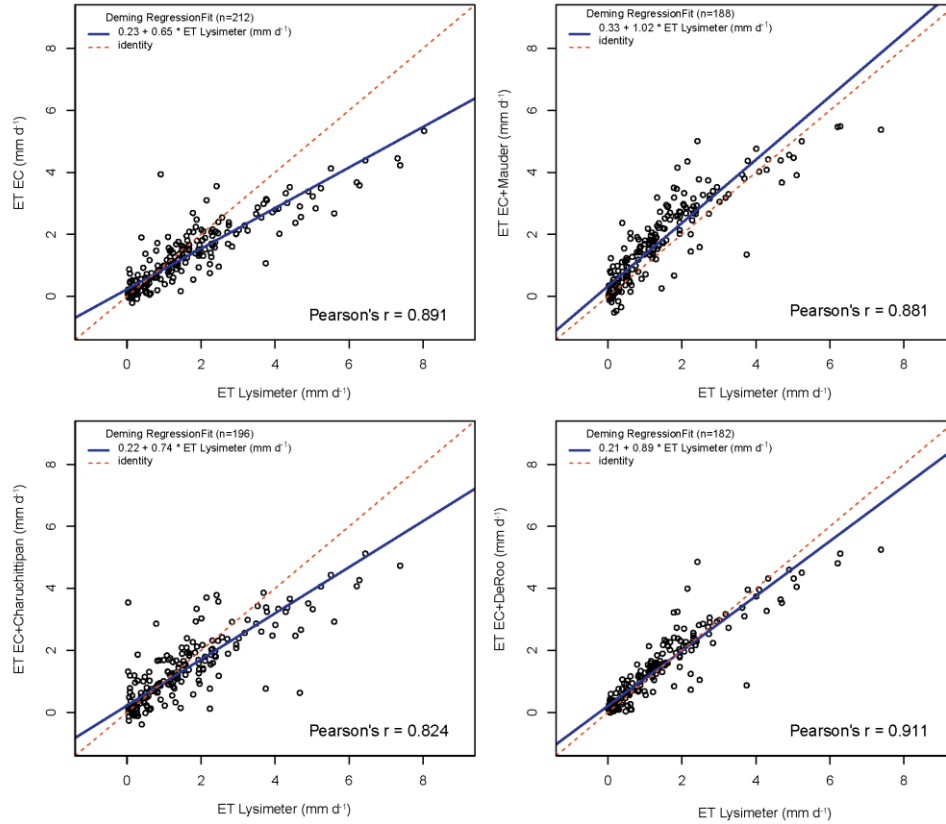
330 **Figure 10: Comparison of daily evapotranspiration (ET) estimates based on eddy-covariance measurements after different variants of energy balance closure correction with daily ET estimates based on lysimeter measurements for the DE-Fen dataset.**

Despite the large difference in terrain complexity between both grassland sites, the results for the DE-Gwg site are quite similar to those for DE-Fen (Figure 11). Again, we find the largest systematic underestimation of ET if no SEB closure correction is applied with a slope of 0.65. We also find the largest scatter and the lowest Pearson's *r* for the method of Charuchittipan et al. (2014) with a value of 0.824 (significance level p < 0.05) and the highest Pearson's *r* for the LES-based method with a value of 0.909911, which is however not significantly improved compared to the uncorrected ET or the method of Mauder et a. (2013). The Bowen-ratio preserving method is slightly overestimating with a slope of 1.02 and an intercept of 0.33 mm d^{-1}, and the LES-based method is slightly underestimating at least for larger ST values with a slope of 0.89 and an intercept of 0.23 mm mm d^{-1}.

Figure 11: Comparison of daily evapotranspiration (ET) estimates based on eddy-covariance measurements after different variants of energy balance closure correction with daily ET estimates based on lysimeter measurements for the DE-Gwg dataset.

Now, after this regression/correlation analysis, we will present the values for comparability and bias, which may provide additional guidance to decide which of the four tested options leads to the best agreement with lysimetric ET estimates. These results are shown in Table 1 and Table 2 for DE-Fen and DE-Gwg. For both datasets, we find a large negative bias of approximately –0.35 mm if no correction is applied, and a roughly equally large positive bias for the Bowen-ratio preserving method. The buoyancy-flux dependent method shows smaller biases than the latter two methods but results in a poorer

18

comparability of 1.40 and 0.855 mm for DE-Fen and DE-Gwg, respectively. Of all four methods, the LES-based correction

leads to the best comparability with values of around 0.5 mm and it also leads to the lowest biases close to zero, i.e. well below

350   0.1 mm per day in absolute numbers.

Table 1: Comparability/root-mean-square error (RMSE) of the different daily ET estimates in mm for the different SEB closure correction methods

RMSE (mm)	No correction (Ingwersen et al., 2011)	Bowen-ratio preserving (Mauder et al., 2013)	Buoyancy-flux dependent (Charuchittipan et al., 2014)	LES-based (De Roo et al., 2018)
DE-Fen	0.811	0.799	1.40	0.551
DE-Gwg	0.858	0.755	0.856	0.561

355

Table 2: Bias/mean error of the different daily ET estimates in mm for the different SEB closure correction methods

Bias (mm)	No correction (Ingwersen et al., 2011)	Bowen-ratio preserving (Mauder et al., 2013)	Buoyancy-flux dependent (Charuchittipan et al., 2014)	LES-based (De Roo et al., 2018)
DE-Fen	−0.365	0.413	-0.064	−0.010
DE-Gwg	−0.346	0.355	-0.184	0.041

4 Discussion

Closure of the SEB is to be expected for any given flux measurement site due to the first law of thermodynamics. A lack of

360   closure indicates that not all assumptions of the EC method are sufficiently fulfilled in reality. Existing partitioning methods

of the SEB residual are either based on no or weak physical basis. The newly proposed method of De Roo et al. (2018) is based

on the understanding of the relevant transport process in the unstable boundary layer. It is well known from numerical and

observational boundary-layer studies that secondary circulations develop under typical daytime conditions, either cell-like or

roll-like depending on the non-local stability parameter z_i/L (Salesky et al., 2017). Both types of large-scale organized

365   structures fill almost the entire boundary layer and contribute to the overall vertical transport of scalars, such as temperature

and humidity, by means of dispersive fluxes. In the presence of roll-like convection, the relative contribution is relatively small

and constant over a wide stability range. As soon as cell-like convection develops, the relative contribution of dispersive fluxes

19

to the total flux increases sharply. Due to differences in typical vertical profiles of these scalars in the boundary layer, relative dispersive fluxes are larger for the transport of sensible heat than for the transport of latent heat in the surface layer (De Roo et al., 2018). No or very small dispersive fluxes are expected for near-neutral or stable stratification because secondary circulations do not develop under those conditions (Jayaraman and Brasseur, 2021). While plausible, this LES-based method has never been validated against real-world data before.

The generally good agreement between this model for dispersive fluxes and the independent reference measurements presented above is encouraging, but is the method of De Roo et al. (2018) really the solution to the longstanding energy balance closure problem? It certainly has the soundest physical basis of all the existing SEB correction approaches, since it is based on the theoretical process understanding that the underestimation of fluxes by single-tower EC systems during daytime is caused by dispersive fluxes that are generated by secondary circulations, and the semi-empirical correction model is the result of a physically-based and systematic LES parameter study. Indeed, its application to the DK-Sor dataset leads to a nearly ideal overall SEB closure. In this case, the magnitude of the dispersive fluxes was modelled directly, and there was no need to use a scaling based on measurements of the available energy at the surface. Therefore, we were able to use these independent measurements of the available energy for validating the magnitude of the predicted SEB residual.

From the comparison of mean diurnal cycles between the modelled dispersive fluxes and the measured residual, we found that the agreement is quite good during the day, meaning that the dispersive fluxes constitute indeed a major part of the missing flux, but during the night, other processes dominate, probably advection and storage terms (e.g. Moderow et al., 2009). Since sensible and latent fluxes are generally small at night, the overall energy balance can still be improved considerably through the correction for dispersive fluxes although these other terms contributing to the residual are not considered. During the summer months, strongly unstable conditions are more frequent and these are associated with cellular convection, which is associated with large dispersive fluxes, while in fall and winter mildly unstable conditions are dominant, which lead to the formation of roll-like secondary circulations, which are associated with smaller dispersive fluxes.

The partitioning of the residual by the method of De Roo et al. (2018) is validated by the comparison of the resulting daily ET rates with independent lysimeter measurements for the DE-Fen and DE-Gwg datasets. The SEB closure after applying this correction is not quite as ideal as for the DK-Sor dataset but still much improved. One reason might be that the imbalance was also initially less at DK-Sor and therefore the absolute correction is higher at the two grassland sites. Nevertheless, the resulting daily ET rates after applying the LES-based correction show the best agreement, i.e. the lowest bias and the lowest RMSE, of the four different methods under investigation when compared with the lysimeter data from both sites. The agreement is very good, despite the difference in scale and methodology between EC and lysimetry. This finding shows that the partitioning by the LES-based method is reasonable, and it is preferable to all other SEB closure adjustment methods that have been published so far. In comparison to the other methods, the RMSE is approximately reduced by 50% through the LES-based method and the bias becomes nearly zero. Hence, this new method is clearly a step forward towards more accurate flux estimates from EC systems which are of critical importance for improving meteorological and ecological models.

However, there are also two main disadvantages of the method by De Roo et al. (2018) that should be discussed. Firstly, this method requires the application of two outlier criteria in order to avoid unrealistic fluxes (see Sect. 3.2). These use somewhat arbitrary and subjective thresholds and they lead to a reduction in data points by 6-7% for the two grassland datasets under study compared to the uncorrected data. However, this only applies to the cases that are limited by z_m. Theoretically, this z_m limitation could be overcome by higher-resolution LES in the future, when this will be computationally feasible. If the correction method is not limited by z_m, as is the case for DK-Sor, no outlier criterium is needed, and hence, no reduction in valid data points can be listed. Secondly, this method was developed from the results of an LES that was driven by homogenous lower boundary conditions and therefore does not include the effects of thermally heterogeneous surface heating on dispersive fluxes, which is relevant under certain realistic conditions as discussed e.g. by Zhou et al. (2019) and Margairaz et al. (2020). Nevertheless, the correction method shows a good comparison with the respective reference measurements for the three test sites, which are far from homogeneous on the landscape scale and also represent different levels of terrain complexity. However, for even more pronounced heterogeneities, especially when they are on a scale of roughly the boundary-layer height or larger, we expect that this method is no longer valid (e.g. Eder et al., 2015).

The only ~~test~~ site tested~~DK-Sor~~, where the correction method can be applied directly (DK-Sor), already has a relatively good SEB closure to begin with. The good closure~~is~~ can be explained by ~~the~~ the rough surface in the surrounding in combination with the relatively high wind velocities that are typical for this region of Denmark. This leads to relatively high values of u_*/w_*, indicating forced convective conditions most of the time. In principle, an additional site with more unstable conditions would be interesting for this study as a complement. However, such sites with high-quality energy-balance data, which also fulfill the criterion of $z_m > 20$ m are scarce. Theoretically, under more strongly unstable conditions, the LES-based correction would be much larger, and also the non-hydrostatic energy transfer might become more relevant (Sun et al., 2021)~~, which otherwise is not the case~~. It is warranted that this correction method is further evaluated, particular for less windy sites with a sufficiently large aerodynamic measurement height, good fetch conditions and high-quality biometeorological measurements. We demonstrated different options how one can deal with the prerequisites for this method, which are an estimate of the boundary-layer height, and for cases that are limited by z_m, matching footprints between the measurement of the different energy balance components and appropriate adaptation of spectral correction methods to the respective instrumentation. The latter two conditions are identical with the prerequisites of high-quality EC measurements in general and can therefore be assumed to be fulfilled after the application of a rigid quality control scheme. However, ~~but in particular,~~ the estimate of the boundary-layer height z_i goes beyond the standard instrumentation of long-term EC sites, although it can also be helpful for other aspects related to long-term flux measurements (Helbig et al., 2021; Wulfmeyer et al., 2020). For a site with flat terrain on the landscape and regional scale, this important nonlocal scaling variable z_i can be modelled from standard in-situ measurements in combination with radio-sounding data that are freely available worldwide. ~~We showed one option for how this important nonlocal scaling variable can be modelled from standard in-situ measurements in combination with radio-sounding data that are freely available worldwide.~~ For study areas that are located in mountainous regions, such as the TERENO Pre-Alpine sites DE-Fen and DE-Gwg, it is advantageous to use ~~actual~~ continuous remote-sensing measurements of

21

435 the z_i by based on ceilometers. Both methods are expected to provide an accuracy on the order of 10% of z_i, which may lead to an error in the energy balance closure of the same magnitude, since it depends linearly on z/z_i. This correction only amounts to 5-30% of the fluxes. Hence, the resulting error of the flux is less than 5-30% of 10%, i.e. 0.5-3%. Moreover, the improvement in the energy balance closure, particularly in reducing the random deviations, shows that both methods work sufficiently well for this purpose.

5 Conclusions

For any operational application of such a method, it needs to be feasible, general and accurate, and our study addresses all of these three aspects. Hence, we presented examples for the application of the novel LES-based SEB closure correction method of De Roo et al. (2018) to three long-term EC sites of different land use and different canopy structure in the mid-latitudes. With respect to the accuracy of the LES-based correction method, we found that it closes SEB almost perfectly on average for
445 the site that is not limited by z_m. For the other two sites, where the application of the correction method is limited by z_m, the resulting bias is also close to zero when comparing the corrected latent heat fluxes with the ET estimate from nearby lysimeters. Not only the accuracy of the flux estimates is improved by this method but also the precision, which is indicated by RMSE values that are reduced by approximately 50%. Hence, our results demonstrate that this method has the potential to be applied for operational application in long-term measurements for many sites around the world. Moreover, these results also suggest
450 that we can simulate the relevant transport processes in the unstable boundary layer realistically with the LES. The general transferability of the idealized LES parameter study of De Roo et al. (2018) to the field has been successfully demonstrated. However, this method is based on assumptions and has some remaining uncertainties. In its current form, it is limited to 30-min block averages for the calculation of fluxes. Moreover, this flux correction method does not account for other sources of bias or SEB non-closure than for the atmospheric transport through dispersive fluxes caused by secondary circulations, which
455 are restricted to unstable conditions. Therefore, it is important to note that storage terms should also be accounted for by an adequate measurement set-up, if they are expected to be significant in magnitude, depending on the depth and the structure of the canopy layer. In addition, great care should be taken in the site selection, the design of the measurement set-up, calibration of the instruments, the implementation of all needed flux corrections and an effective set of quality control procedures (Mauder et al., 2021), because this SEB closure correction cannot account for any of these aspects.
460 The promising results of this study will hopefully encourage further validation of this LES-based method for other sites around the world, which perhaps even allow for a combined testing of magnitude and partitioning of the correction. It also remains to be evaluated at what level of surface heterogeneity this method starts to lead to unrealistic results. We expect such a failure of this method that was derived from completely homogeneous LES runs to occur when the formation of secondary circulations is dominated by surface heterogeneity rather than self-organization of turbulence. In such cases, a set of LES runs that are
465 representative for a specific heterogeneous measurement site could potentially be used to overcome this limitation. Further

investigations are also warranted to establish whether a similar SEB closure correction could also be applicable for other trace gases and scalars, e.g. CO_2.

480   **References**

Aubinet, M., Grelle, A., Ibrom, A., Rannik, U., Moncrieff, J., Foken, T., Kowalski, A. S., H., M. P., Berbigier, P., Bernhofer, C., Clement, R., Elbers, J., Granier, A., Grünwald, T., K., M., K., P., C., R., W., S., Valentini, R. and Vesala, T.: Estimates of the annual net carbon and water exchange of forest: the EUROFLUX methodology, Adv. Ecol. Res., 30, 113–117, doi:10.1016/S0065-2504(08)60018-5, 2000.

485   Aubinet, M., Vesala, T. and Papale, D., Eds.: Eddy Covariance - A Practical Guide to Measurement and Data Analysis, Springer, Dordrecht., 2012.

Batchvarova, E. and Gryning, S.-E.: Applied Model for the Growth of the Daytime Mixed Layer, Boundary-Layer Meteorol., 56, 261–274, doi:10.1007/BF00120423, 1991.

Charuchittipan, D., Babel, W., Mauder, M., Leps, J.-P. and Foken, T.: Extension of the Averaging Time in Eddy-Covariance

490   Measurements and Its Effect on the Energy Balance Closure, Boundary-Layer Meteorol., 152(3), 303–327, doi:10.1007/s10546-014-9922-6, 2014.

Eder, F., De Roo, F., Rotenberg, E., Yakir, D., Schmid, H. P. and Mauder, M.: Secondary circulations at a solitary forest surrounded by semi-arid shrubland and its impact on eddy-covariance measurements, Agric. For. Meteorol., 211–212, 115–127, doi:10.1016/j.agrformet.2015.06.001, 2015.

495   Emeis, S., Schäfer, K., Münkel, C., Friedl, R. and Suppan, P.: Evaluation of the Interpretation of Ceilometer Data with RASS and Radiosonde Data, Boundary-Layer Meteorol., 143(1), 25–35 [online] Available from: http://dx.doi.org/10.1007/s10546-011-9604-6, 2011.

23

Etling, D. and Brown, R. A.: Roll vortices in the planetary boundary layer: A review, Boundary-Layer Meteorol., 65(3), 215–248 [online] Available from: http://dx.doi.org/10.1007/BF00705527, 1993.

500 Foken, T. and Wichura, B.: Tools for quality assessment of surface-based flux measurements, Agric. For. Meteorol., 78, 83–105, 1996.

Foken, T., Göckede, M., Mauder, M., Mahrt, L., Amiro, B. and Munger, W.: Post-field data quality control, in Handbook of Micrometeorology. A Guide for Surface Flux Measurement and Analysis, edited by X. Lee, W. Massman, and Law. Beverly, pp. 181–208, Kluwer Academic Publishers, Dordrecht., 2004.

505 Fu, J., Gasche, R., Wang, N., Lu, H., Butterbach-Bahl, K. and Kiese, R.: Impacts of climate and management on water balance and nitrogen leaching from three montane grassland soils in S-Germany, Environ. Pollut., 229, 119–131, doi:10.1016/j.envpol.2017.05.071, 2017.

Helbig, M., Gerken, T., Beamesderfer, E., Baldocchi, D. D., Banerjee, T., Biraud, S. C., Brown, W. O. J., Brunsell, N. A., Burakowski, E. A., Burns, S. P., Butterworth, B. J., Chan, W. S., Davis, K. J., Desai, A. R., Fuentes, J. D., Hollinger, D. Y.,

510 Kljun, N., Mauder, M., Novick, K. A., Perkins, J. M., Rahn, D. A., Rey-Sanchez, C., Santanello, J. A., Scott, R. L., Seyednasrollah, B., Stoy, P. C., Sullivan, R. C., Arellano, J. V.-G. de, Wharton, S., Yi, C. and Richardson, A. D.: Integrating continuous atmospheric boundary layer and tower-based flux measurements to advance understanding of land-atmosphere interactions, Agric. For. Meteorol., 307, 108509, doi:10.1016/j.agrformet.2021.108509, 2021.

Hendricks-Franssen, H. J., Stöckli, R., Lehner, I. and Seneviratne, S. I.: Analysis of the energy balance closure as function of

515 atmospheric stability and wind velocity at 27 European FLUXNET sites, Assembly, 11, 10339, 2009.

Inagaki, A., Letzel, M. O., Raasch, S. and Kanda, M.: Impact of surface heterogeneity on energy imbalance, J. Meteorol. Soc. Japan, 84(1), 187–198, 2006.

Ingwersen, J., Steffens, K., Högy, P., Warrach-Sagi, K., Zhunusbayeva, D., Poltoradnev, M., Gäbler, R., Wizemann, H.-D. D., Fangmeier, a., Wulfmeyer, V. and Streck, T.: Comparison of Noah simulations with eddy covariance and soil water

520 measurements at a winter wheat stand, Agric. For. Meteorol., 151(3), 345–355, doi:10.1016/j.agrformet.2010.11.010, 2011.

Jayaraman, B. and Brasseur, J. G.: Transition in atmospheric boundary layer turbulence structure from neutral to convective, and large-scale rolls, J. Fluid Eng., 1–31, doi:10.1017/jfm.2021.3, 2021.

Kaimal, J. C. C. and Finnigan, J. J.: Atmospheric Boundary Layer Flows: Their Structure and Measurement, Oxford University Press, New York., 1994.

525 Kanda, M., Inagaki, A., Letzel, M. O., Raasch, S. and Watanabe, T.: LES study of the energy imbalance problem with eddy covariance fluxes, Boundary-Layer Meteorol., 110(3), 381–404, 2004.

Kiese, R., Fersch, B., Baessler, C., Brosy, C., Butterbach-Bahl, K., Chwala, C., Dannenmann, M., Fu, J., Gasche, R., Grote, R., Jahn, C., Klatt, J., Kunstmann, H., Mauder, M., Rödiger, T., Smiatek, G., Soltani, M., Steinbrecher, R., Völksch, I., Werhahn, J., Wolf, B., Zeeman, M. and Schmid, H. P.: The TERENO Pre-Alpine Observatory: Integrating Meteorological,

530 Hydrological, and Biogeochemical Measurements and Modeling, Vadose Zo. J., 17, 180060, doi:10.2136/vzj2018.03.0060, 2018.

Kljun, N., Calanca, P., Rotach, M. W. and Schmid, H. P.: A simple two-dimensional parameterisation for Flux Footprint Prediction (FFP), Geosci. Model Dev., 8(11), 3695–3713, doi:10.5194/gmd-8-3695-2015, 2015.

Lee, X.: Fundamentals of Boundary-Layer Meteorology, Springer Atmospheric Sciences., 2018.

535 Liebethal, C., Huwe, B. and Foken, T.: Sensitivity analysis for two ground heat flux calculation approaches, Agric. For. Meteorol., 132, 253–262, doi:10.1016/j.agrformet.2005.08.001, 2005.

Manuilova, E., Schuetzenmeister, A. and Model, F.: mcr: Method Comparison Regression, [online] Available from: https://cran.r-project.org/package=mcr, 2014.

Margairaz, F., Pardyjak, E. R. and Calaf, M.: Surface thermal heterogeneities and the atmospheric boundary layer: the
540 relevance of dispersive fluxes, Boundary-Layer Meteorol., 175, 369–395, doi:10.1007/s10546-020-00509-w, 2020.

Mauder, M., Cuntz, M., Drüe, C., Graf, A., Rebmann, C., Schmid, H. P., Schmidt, M. and Steinbrecher, R.: A strategy for quality and uncertainty assessment of long-term eddy-covariance measurements, Agric. For. Meteorol., 169, 122–135, doi:10.1016/j.agrformet.2012.09.006, 2013.

Mauder, M., Genzel, S., Fu, J., Kiese, R., Soltani, M., Steinbrecher, R., Kunstmann, H., Zeeman, M., Banerjee, T., De Roo,
545 F., Kunstmann, H. and Zeeman, M.: Evaluation of energy balance closure adjustment methods by independent evapotranspiration estimates from lysimeters and hydrological simulations, Hydrol. Process., 32(October), 39–50, doi:10.1002/hyp.11397, 2018.

Mauder, M., Foken, T. and Cuxart, J.: Surface energy balance closure over land: a review, Boundary-Layer Meteorol., (177), 395–426, doi:10.1007/s10546-020-00529-6, 2020.

550 Mauder, M., Foken, T., Aubinet, M. and Ibrom, A.: Eddy-covariance measurements, in Springer Handbook of Atmospheric Measurements, edited by T. Foken, pp. 1493–1542, in press, Springer Nature Switzerland., 2021.

Moderow, U., Aubinet, M., Feigenwinter, C., Kolle, O., Lindroth, A., Mölder, M., Montagnani, L., Rebmann, C. and Bernhofer, C.: Available energy and energy balance closure at four coniferous forest sites across Europe, Theor. Appl. Climatol., 98, 397–412, 2009.

555 Moore, C. J.: Frequency response corrections for eddy correlation systems, Boundary-Layer Meteorol., 37(1–2), 17–35, doi:10.1007/BF00122754, 1986.

Münkel, C., Eresmaa, N., Räsänen, J. and Karppinen, A.: Retrieval of mixing height and dust concentration with lidar ceilometer, Boundary-Layer Meteorol., 124(1), 117–128, doi:10.1007/s10546-006-9103-3, 2007.

Peters, A., Nehls, T., Schonsky, H. and Wessolek, G.: Separating precipitation and evapotranspiration from noise – a new filter
560 routine for high-resolution lysimeter data, Hydrol. Earth Syst. Sci., 18, 1189–1198, doi:10.5194/hess-18-1189-2014, 2014.

Pilegaard, K. and Ibrom, A.: Net carbon ecosystem exchange during 24 years in the Sorø Beech Forest – relations to phenology and climate, Tellus B Chem. Phys. Meteorol., 72(1), 1–17, doi:10.1080/16000889.2020.1822063, 2020.

Pütz, T., Kiese, R., Wollschläger, U., Groh, J., Rupp, H., Zacharias, S., Priesack, E., Gerke, H. H., Gasche, R., Bens, O., Borg, E., Baessler, C., Kaiser, K., Herbrich, M., Munch, J. C., Sommer, M., Vogel, H. J., Vanderborght, J. and Vereecken, H.:
565 TERENO-SOILCan: a lysimeter-network in Germany observing soil processes and plant diversity influenced by climate

25

change, Environ. Earth Sci., 75(1242), doi:10.1007/s12665-016-6031-5, 2016.

Reichstein, M., Falge, E., Baldocchi, D., Papale, D., Aubinet, M., Berbigier, P., Bernhofer, C., Buchmann, N., Gilmanov, T., Granier, A., Grunwald, T., Havrankova, K., Ilvesniemi, H., Janous, D., Knohl, A., Laurila, T., Lohila, A., Loustau, D., Matteucci, G., Meyers, T., Miglietta, F., Ourcival, J.-M. M., Pumpanen, J., Rambal, S., Rotenberg, E., Sanz, M., Tenhunen, J., Seufert, G., Vaccari, F., Vesala, T., Yakir, D. and Valentini, R.: On the separation of net ecosystem exchange into assimilation and ecosystem respiration: review and improved algorithm, Glob. Chang. Biol., 11(9), 1424–1439, doi:10.1111/j.1365-2486.2005.001002.x, 2005.

De Roo, F., Zhang, S., Huq, S. and Mauder, M.: A semi-empirical model of the energy balance closure in the surface layer, PLoS One, 13(12), e0209022, doi:10.1371/journal.pone.0209022, 2018.

Ruppert, J., Mauder, M., Thomas, C. and Lüers, J.: Innovative gap-filling strategy for annual sums of CO_2 net ecosystem exchange, Agric. For. Meteorol., 138(1–4), doi:10.1016/j.agrformet.2006.03.003, 2006.

Sabbatini, S., Mammarella, I., Arriga, N., Fratini, G., Graf, A., Hörtnagl, L., Ibrom, A., Longdoz, B., Mauder, M., Merbold, L., Metzger, S., Montagnani, L., Pitacco, A., Rebmann, C., Sedlák, P., Sigut, L., Vitale, D. and Papale, D.: Eddy covariance raw data processing for CO2 and energy fluxes calculation at ICOS ecosystem stations, Int. Agrophysics, 32, 495–515, doi:10.1515/intag-2017-0043, 2018.

Salesky, S. T., Chamecki, M. and Bou-Zeid, E.: On the Nature of the Transition Between Roll and Cellular Organization in the Convective Boundary Layer, Boundary-Layer Meteorol., 163(1), 41–68, doi:10.1007/s10546-016-0220-3, 2017.

Schotanus, P., Nieuwstadt, F. T. M. and DeBruin, H. A. R.: Temperature measurement with a sonic anemometer and its application to heat and moisture fluctuations, Boundary-Layer Meteorol., 26, 81–93, 1983.

Soltani, M., Mauder, M., Laux, P. and Kunstmann, H.: Turbulent flux variability and energy balance closure in the TERENO prealpine observatory: a hydrometeorological data analysis, Theor. Appl. Climatol., 133(3), 937–956, doi:10.1007/s00704-017-2235-1, 2018.

Steinfeld, G., Letzel, M. O., Raasch, S., Kanda, M. and Inagaki, A.: Spatial representativeness of single tower measurements on the imbalance problem with eddy-covariance fluxes: results of a large-eddy simulation study, Boundary-Layer Meteorol., 123(1), 77–98, 2007.

Stoy, P. C., Mauder, M., Foken, T., Marcolla, B., Boegh, E., Ibrom, A., Arain, M. A. A., Arneth, A., Aurela, M., Bernhofer, C., Cescatti, A., Dellwik, E., Duce, P., Gianelle, D., van Gorsel, E., Kiely, G., Knohl, A., Margolis, H., Mccaughey, H., Merbold, L., Montagnani, L., Papale, D., Reichstein, M., Saunders, M., Serrano-Ortiz, P., Sottocornola, M., Spano, D., Vaccari, F. and Varlagin, A.: A data-driven analysis of energy balance closure across FLUXNET research sites: The role of landscape-scale heterogeneity, Agric. For. Meteorol., 171–172, 137–152, doi:10.1016/j.agrformet.2012.11.004, 2013.

Sun, J., Massman, W. J., Banta, R. M. and Burns, S. P.: Revisiting the Surface Energy Imbalance, J. Geophys. Res. Atmos., 126, e2020JD034219, doi:10.1029/2020jd034219, 2021.

Twine, T. E., Kustas, W. P., Norman, J. M., Cook, D. R., Houser, P. R., Meyers, T. P., Prueger, J. H., Starks, P. J. and Wesely, M. L.: Correcting eddy-covariance flux underestimates over a grassland, Agric. For. Meteorol., 103(3), 279–300,

600   doi:10.1016/S0168-1923(00)00123-4, 2000.

Webb, E. K., Pearman, G. I. and Leuning, R.: Correction of the flux measurements for density effects due to heat and water vapour transfer, Q. J. R. Meteorol. Soc., 106, 85–100, 1980.

Wilson, K., Goldstein, A., Falge, E., Aubinet, M., Baldocchi, D., Berbigier, P., Bernhofer, C., Ceulemans, R., Dolman, H. and Field, C.: Energy balance closure at FLUXNET sites, Agric. For. Meteorol., 113(1–4), 223–243, doi:10.1016/S0168-

605   1923(02)00109-0, 2002.

Wohlfahrt, G., Irschick, C., Thalinger, B., Hörtnagl, L., Obojes, N., Hammerle, A., Hortnagl, L., Obojes, N. and Hammerle, A.: Insights from independent evapotranspiration estimates for closing the energy balance: a grassland case study, Vadose Zo. J., 9(4), 1025–1033, doi:10.2136/vzj2009.0158, 2010.

Wulfmeyer, V., Späth, F., Behrendt, A., Jach, L., Warrach-Sagi, K., Ek, M., Turner, D., Senff, C., Ferguson, C., Santanello,

610   J., Lee, T., Buban, M. and Verhoef, A.: The GEWEX Land-Atmosphere Feedback Observatory (GLAFO), GEWEX Q., 30(1), 6–11, doi:10.1002/wat2.1172.Table, 2020.

Wutzler, T., Lucas-Moffat, A., Migliavacca, M., Knauer, J., Sickel, K., Šigut, L., Menzer, O. and Reichstein, M.: Basic and extensible post-processing of eddy covariance flux data with REddyProc, Biogeosciences, 15, 5015–5030, doi:10.5194/bg-15-5015-2018, 2018.

615   Zhou, Y., Li, D. and Li, X.: The Effects of Surface Heterogeneity Scale on the Flux Imbalance under Free Convection, JGR Atmos., 124(15), 8424–8448, doi:10.1029/2018JD029550, 2019.